Modeling impurity distribution in an ST using a transmission grating based diagnostic in the EUV range

D. Kumar, D. Stutman, K. Tritz, D. Clayton, M. Finkenthal
Plasma Spectroscopy Group,
Department of Physics and Astronomy,
The Johns Hopkins University.

Motivation

- The Transmission Grating Imaging Spectrometer (TGIS) forms a diagnostic suite with the Multi Energy Soft Xray (MESXR BP9.00086) system with the following capabilities
  - Model impurity fractions from edge to core, providing spatial distribution over a wide range of plasma temperatures
  - Ability to observe radiation from low Z, medium Z and high Z impurities.
  - Also measures charge exchange signals from low Z impurities
  - Has a very simple design
- This poster highlights the capability of TGIS and also illustrates the modeling of relative impurity fractions

The diagnostic suite – TGIS + MESXR

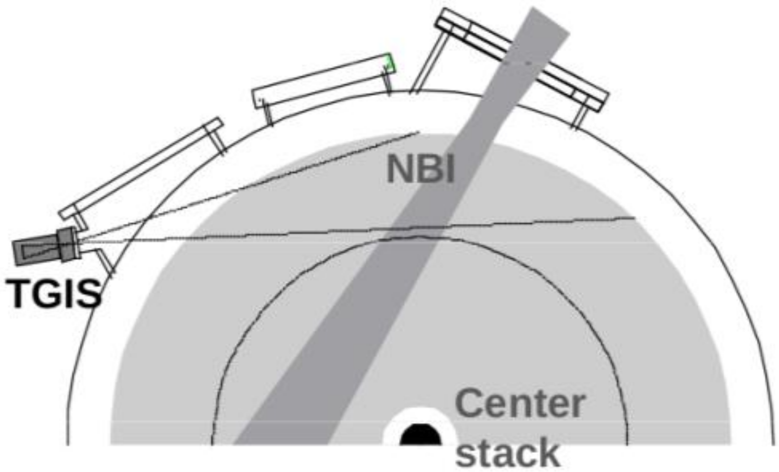

NSTX mid plane view of TGIS

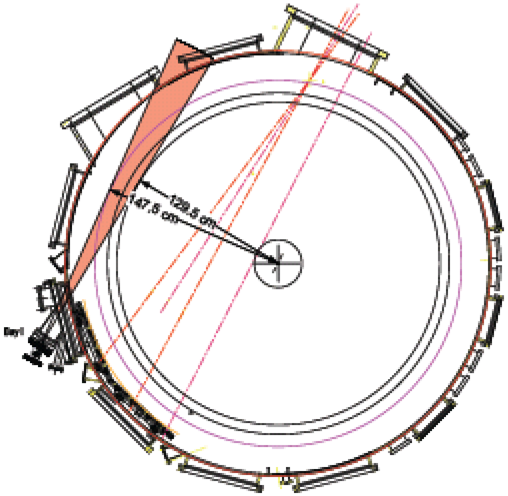

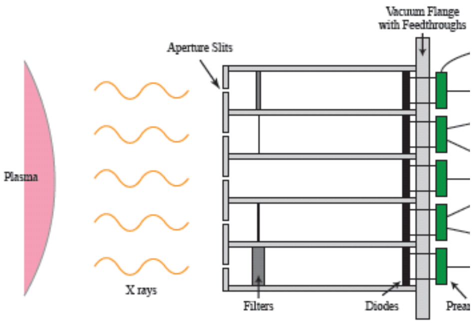

Schematic of MESXR measuring edge/core emission by filtered diodes

TGIS setup

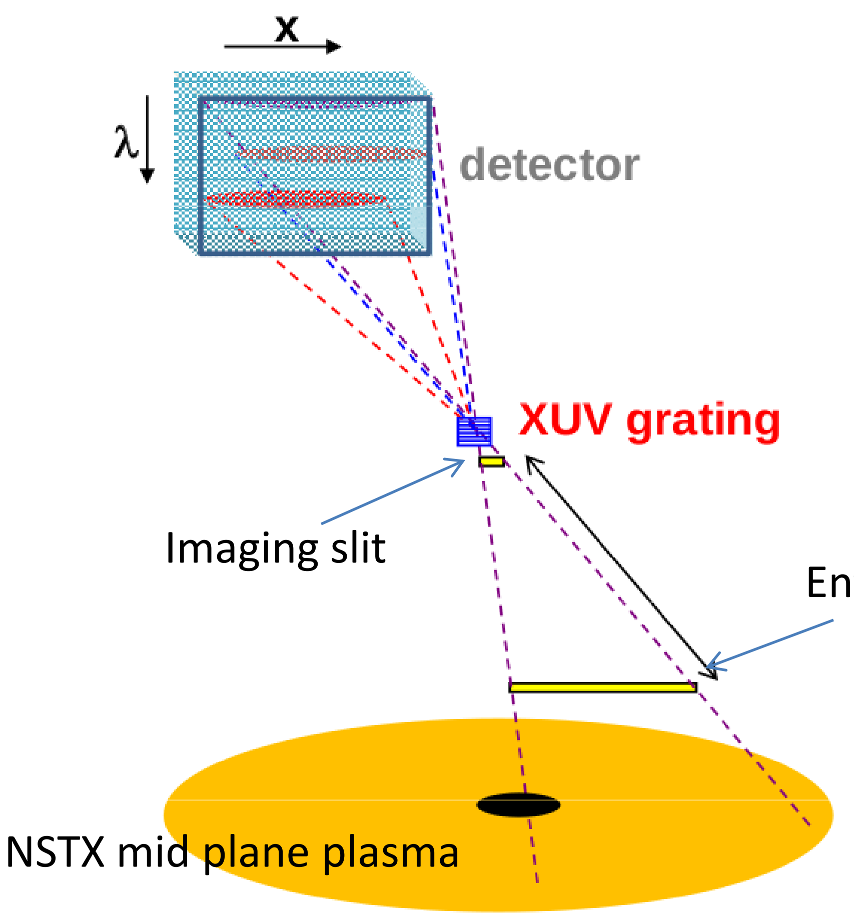
x
λ
detector
XUV grating
Imaging slit
NSTX mid plane plasma

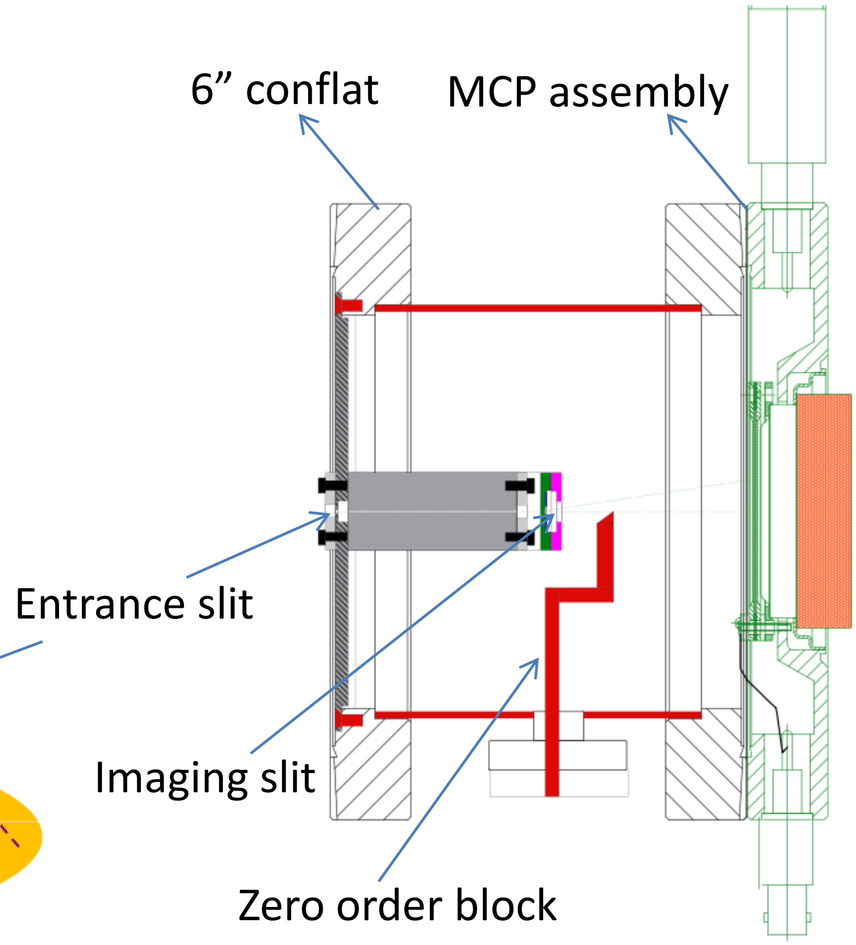
6" conflat
MCP assembly
Entrance slit
Imaging slit
Zero order block

Device Setup

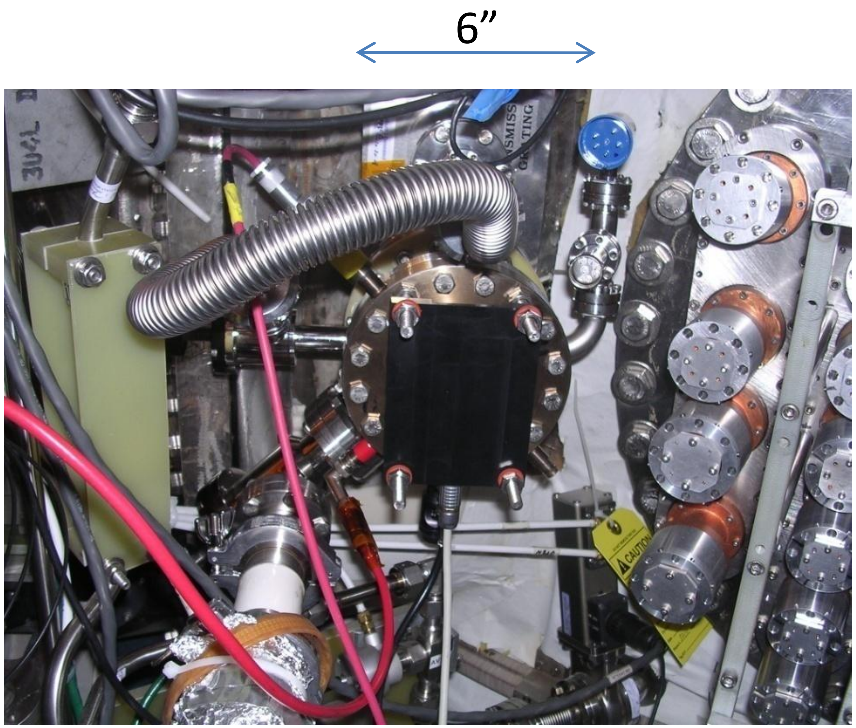

TGIS installed on NSTX

- Detection
  - CsI coated MCP
  - Phosphor screen
  - CMOS imaging system (380 ms exposure)
- Design advantages
  - Survey spectrometer
    (50-700 Å)
  - Robust to neutrons
  - Provides spatial impurity distribution
  - Simple and compact

Grating details

- Free standing transmission grating (NTT-AT ATN/TG-200/11W)
  - Dimensions: 1 mm x 1 mm
  - 5000 lines/mm

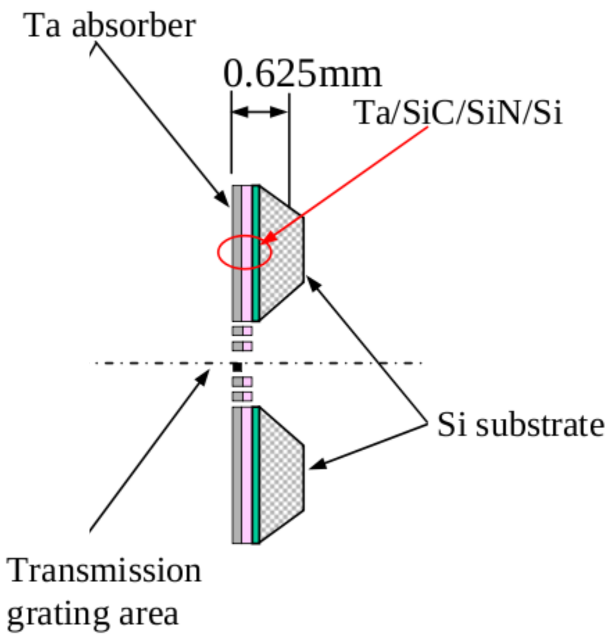

SEM image of the transmission grating area

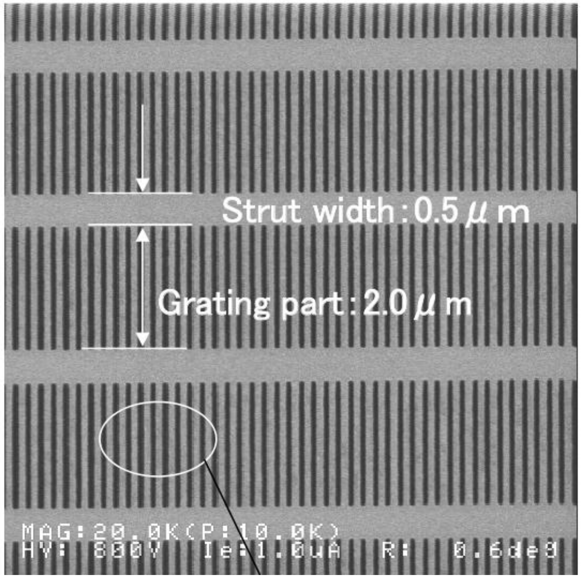

Efficiency calibrations

- NIST grating calibrations

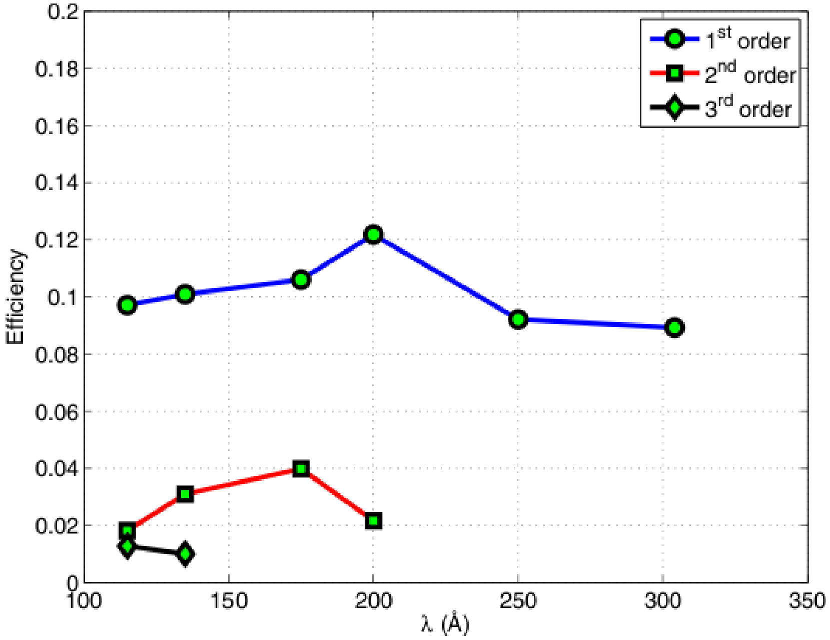

- Expected MCP gain variation

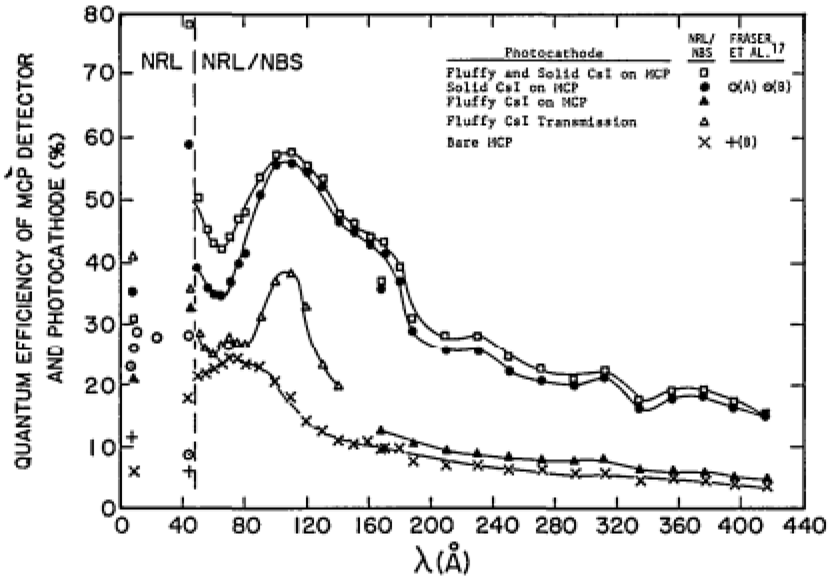

Kowalski et. al, Applied Optics (1986)

Wavelength calibration using a Penning discharge

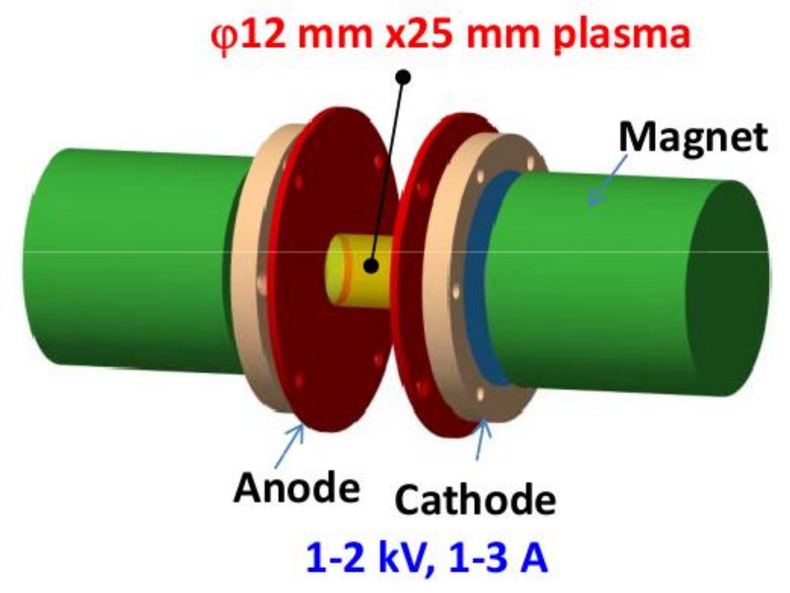

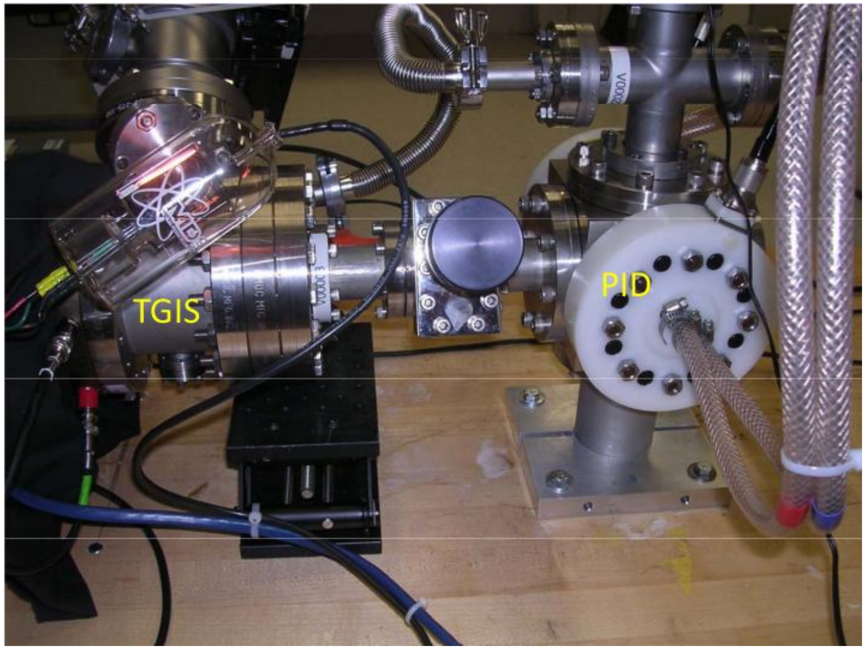

Absolute calibration of TGIS will be done by using Andor iKon-M camera as detector

Wavelength calibration using a Penning discharge

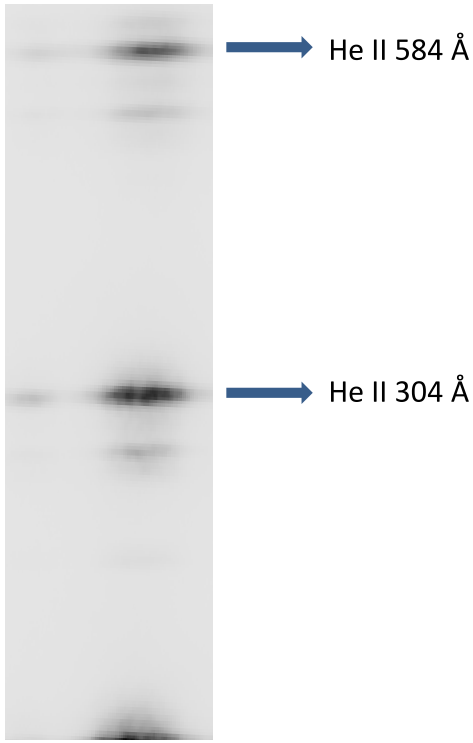

He gas + Al cathodes

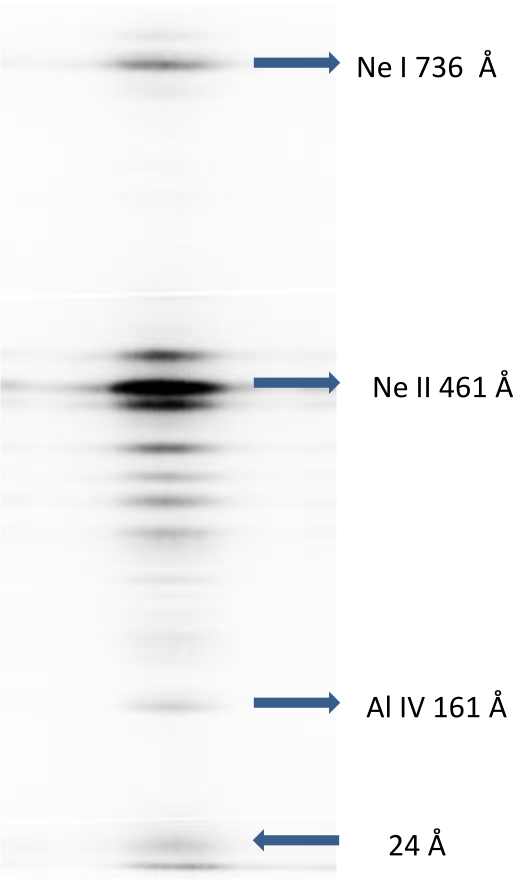

Ne gas + Al cathodes

Spectra from NBI heated plasma

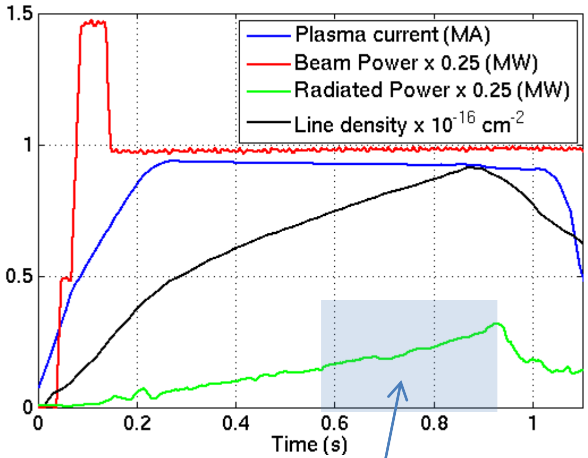

Exposure time of spectra

Traces of Cl

CX signals

Shot: 142192

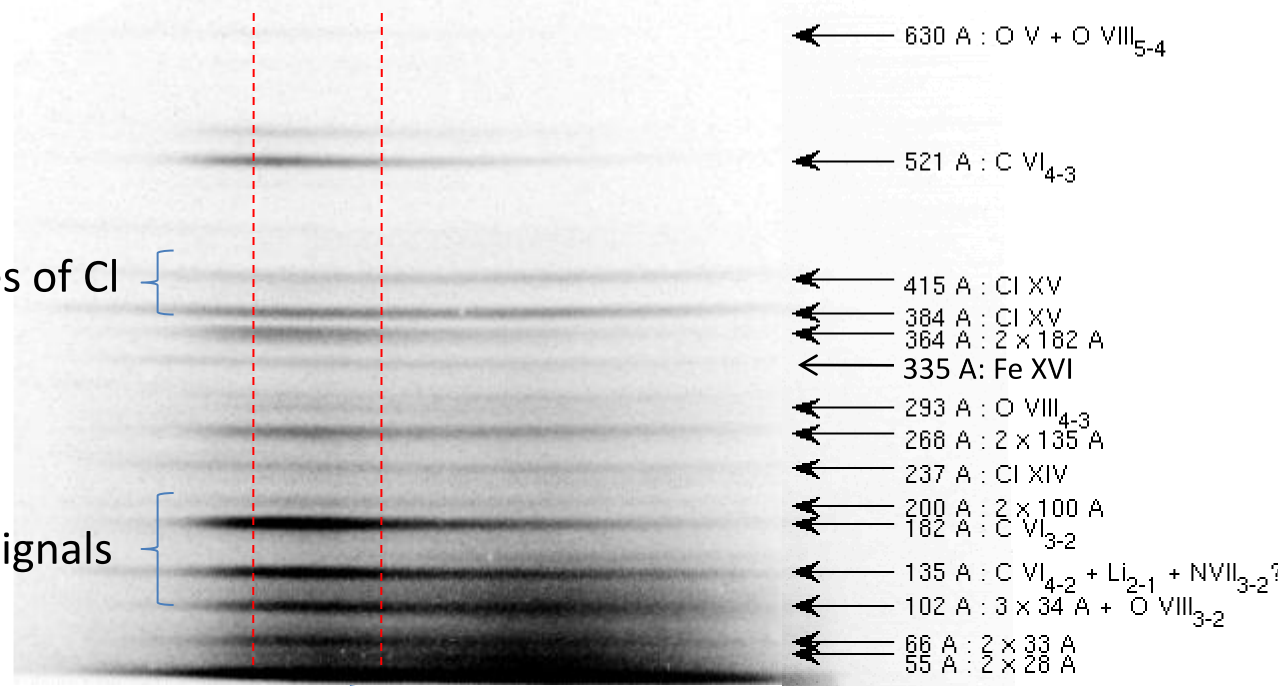

Region of intense beam interaction

- Spectra is dominated by low Z CX signals.
- With traces of Cl

TGIS is a sensitive monitor of med Z impurity accumulation in the core

The radiated power is very high because of impurity accumulation

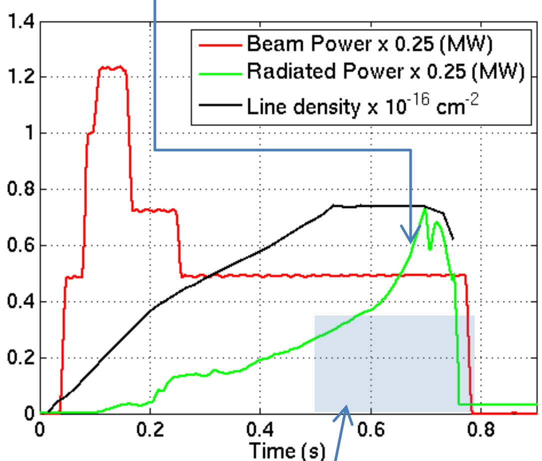

Exposure time of spectra

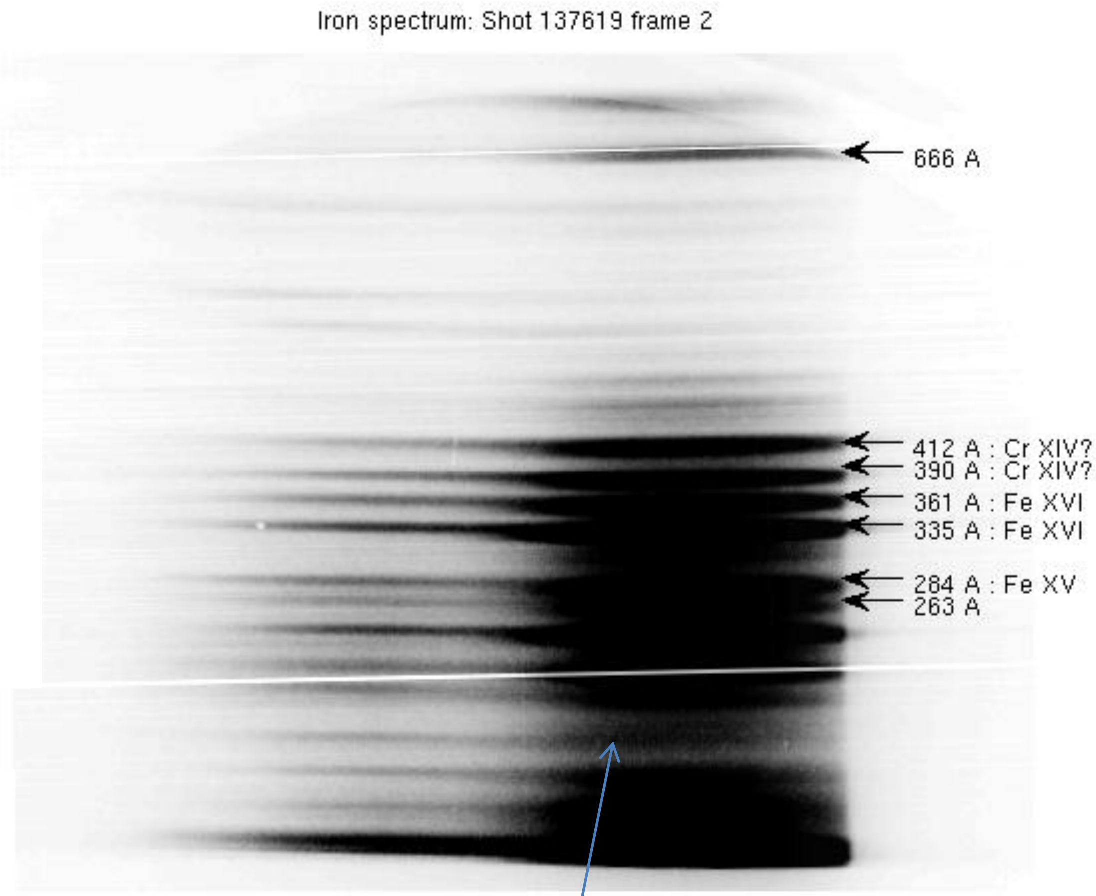

Accumulation in the core

Spectra obtained from ohmic shot

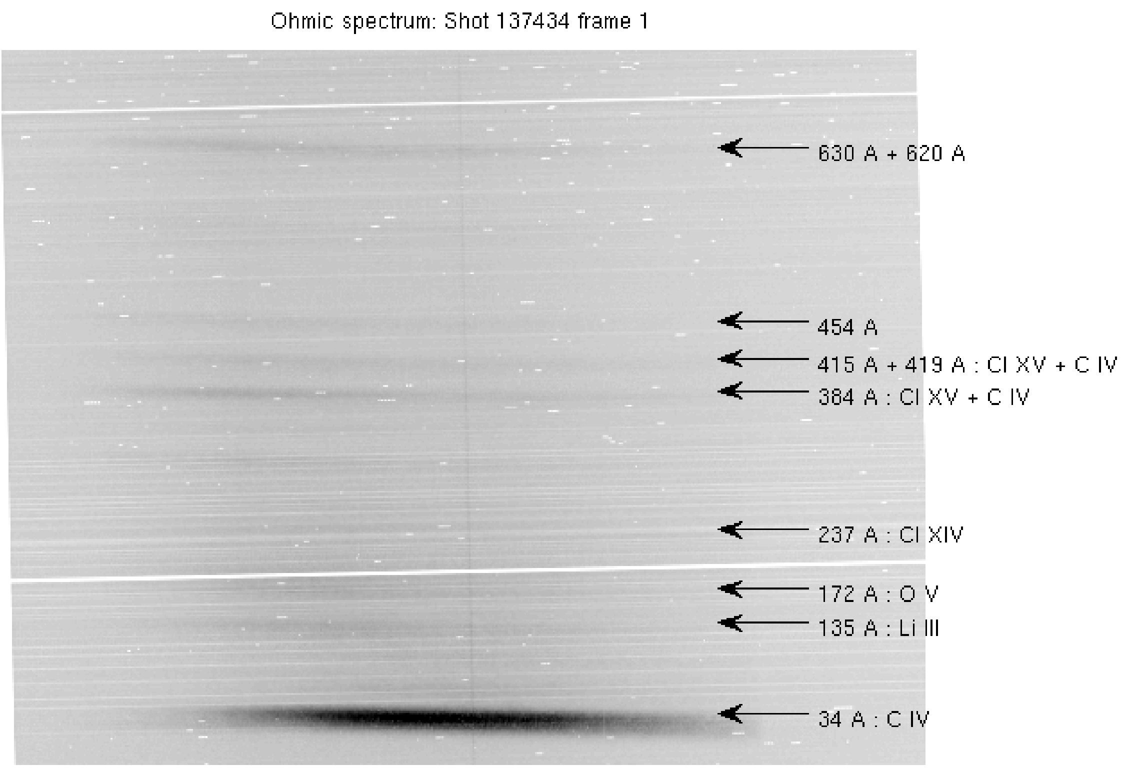

- Spectra from ohmic shots is dominated by edge emissions
- It confirms the interpretation of low Z charge exchange lines in NBI heated shots

Spectra of high Z impurity - Tungsten

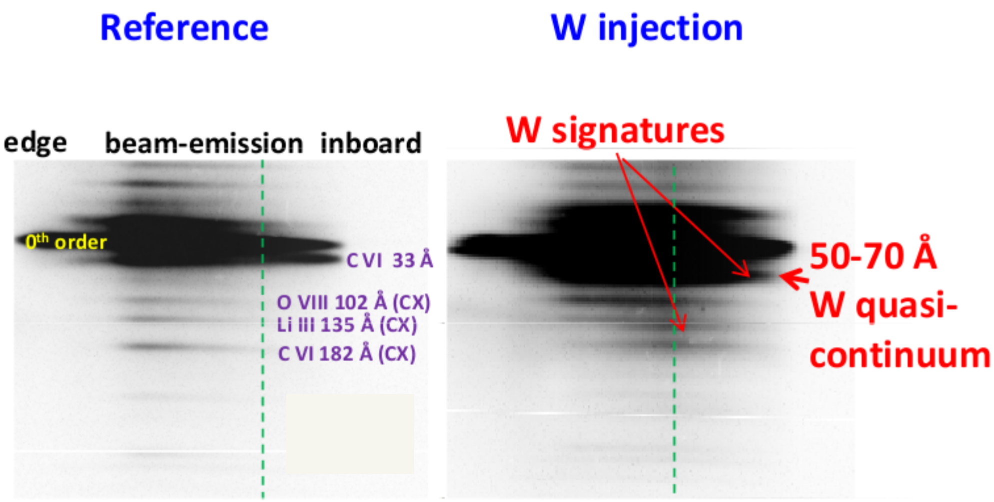

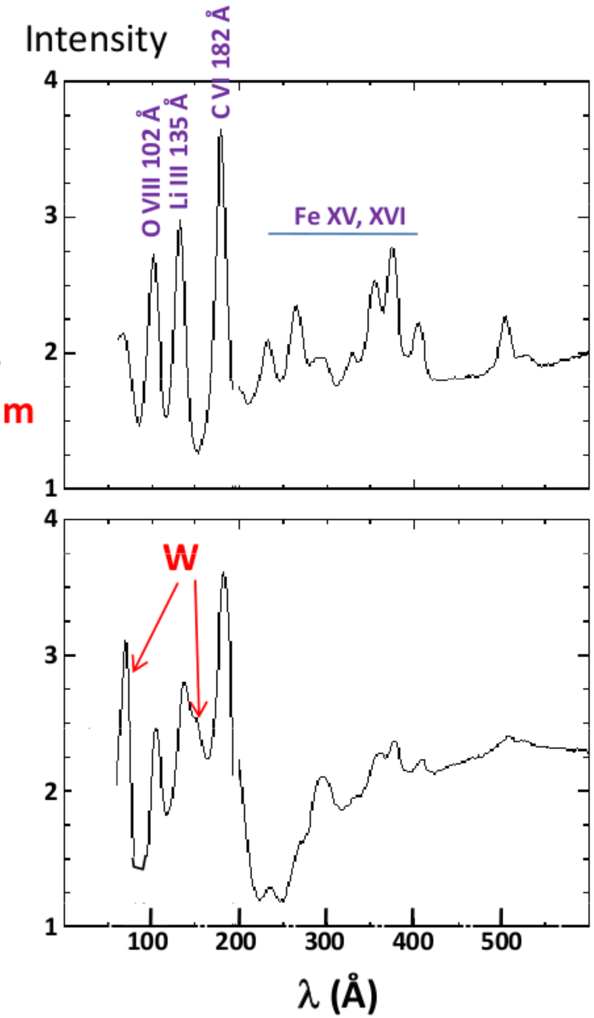

Model for TGIS charge exchange emission

- Neutral beam density modeled for each beam (and each component). Attenuation of different beam components is illustrated

Path length along beam

$$n_n(x) = n_\circ e^{-\sigma l n_e}$$

Neutral density from each beam component

Stopping cross section

A Gaussian profile is assumed for each beam

Coefficients from Janev et. al. Nuclear Fusion (1989)

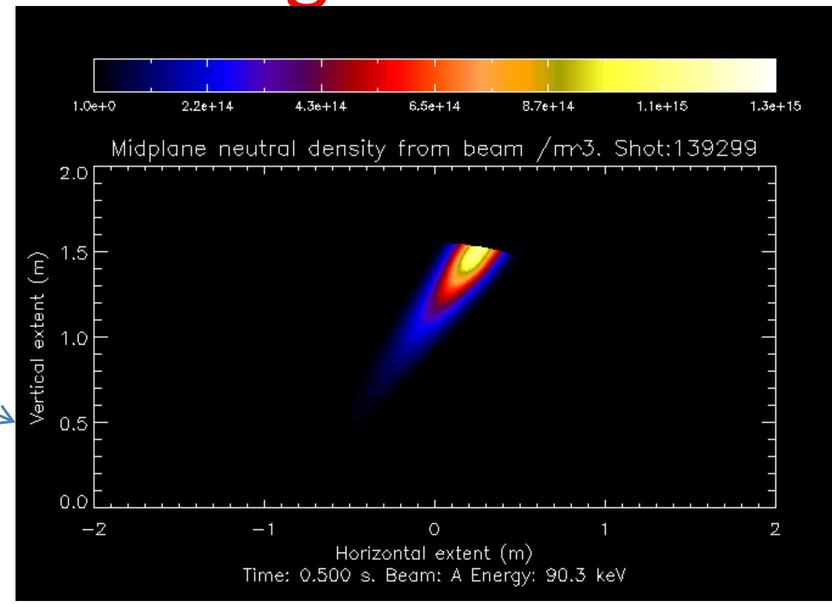

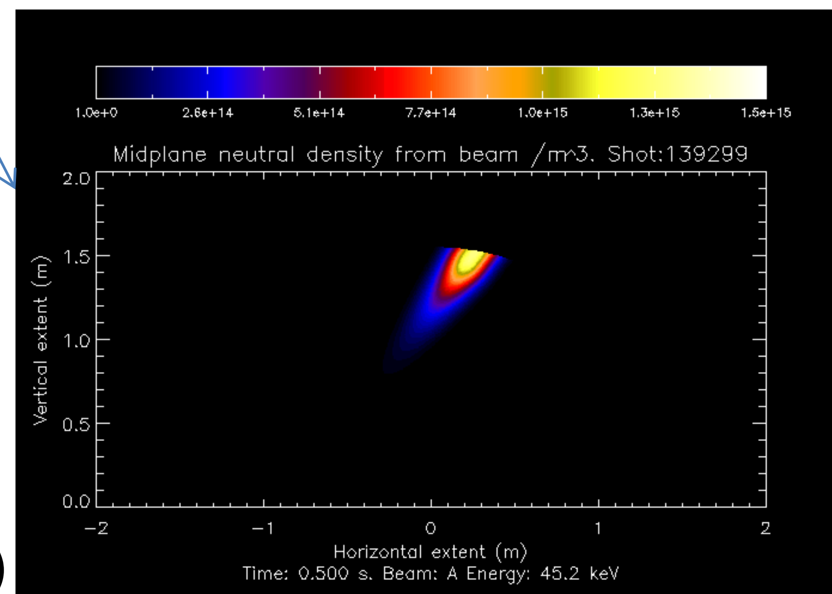

Calculation of C charge exchange emissivity

Neutral beam density

Carbon density (obtained from CHERS)

Neutral velocity

$$E(x) = n_C \sum_i n_{n_i} \sigma_i v_i$$

Emissivity

CX cross section

Sum over beam components

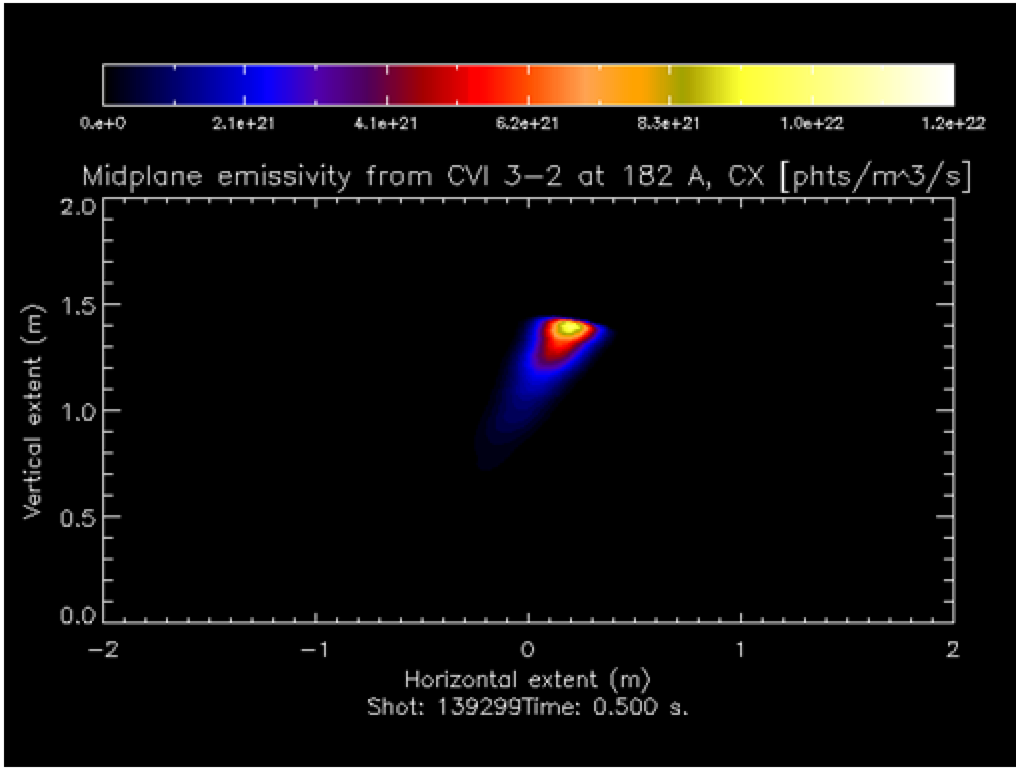

The model successfully predicts the spatial profile of brightness of CX lines

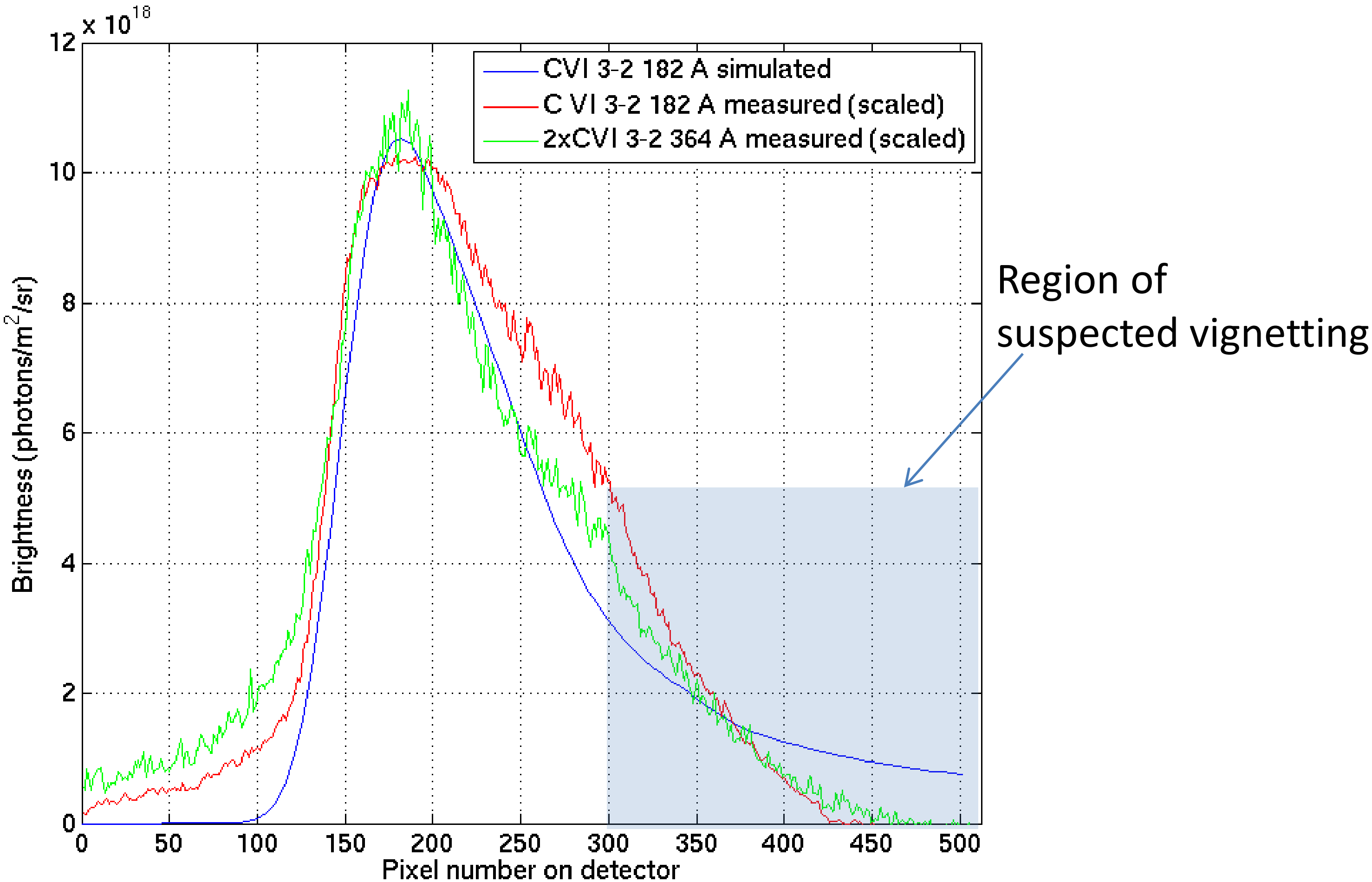

Charge exchange coefficients obtained from Isler (1994), Isler and Langley (1985)

Charge exchange brightness strongly dominates collisional excitation for non-resonant lines

- Representative simulated examples of C and O shown below.

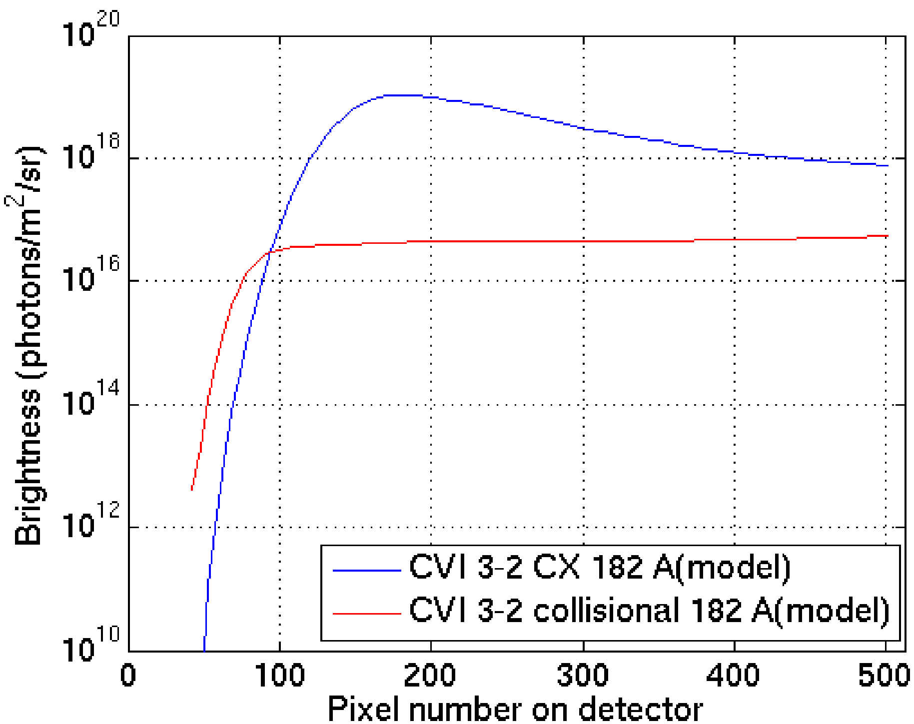

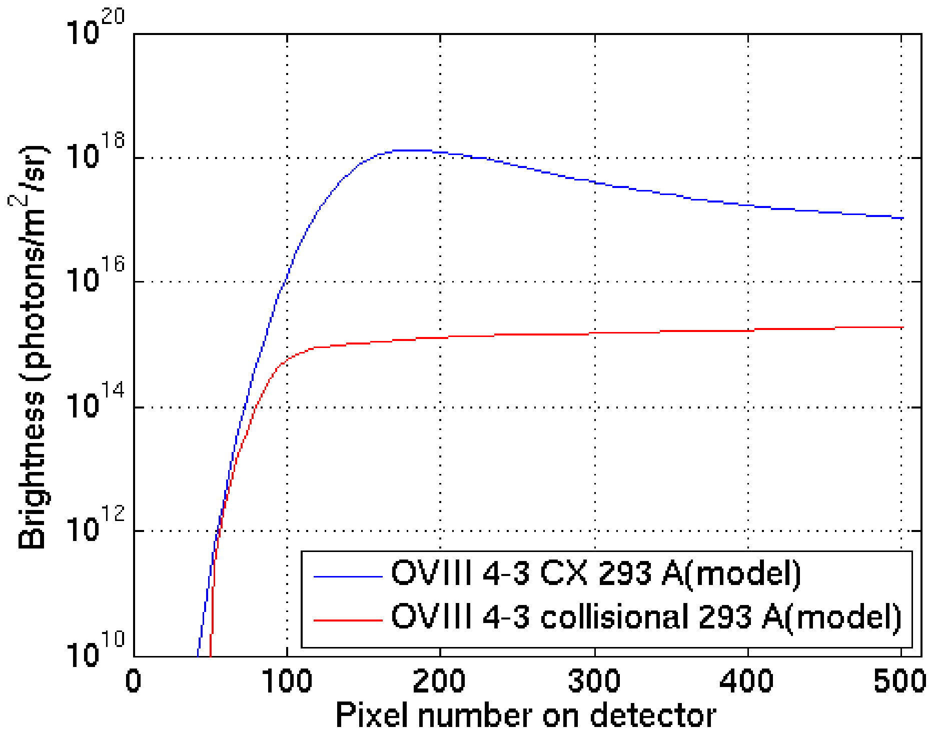

For resonant transitions – brightness from collisional excitation is comparable to brightness from CX

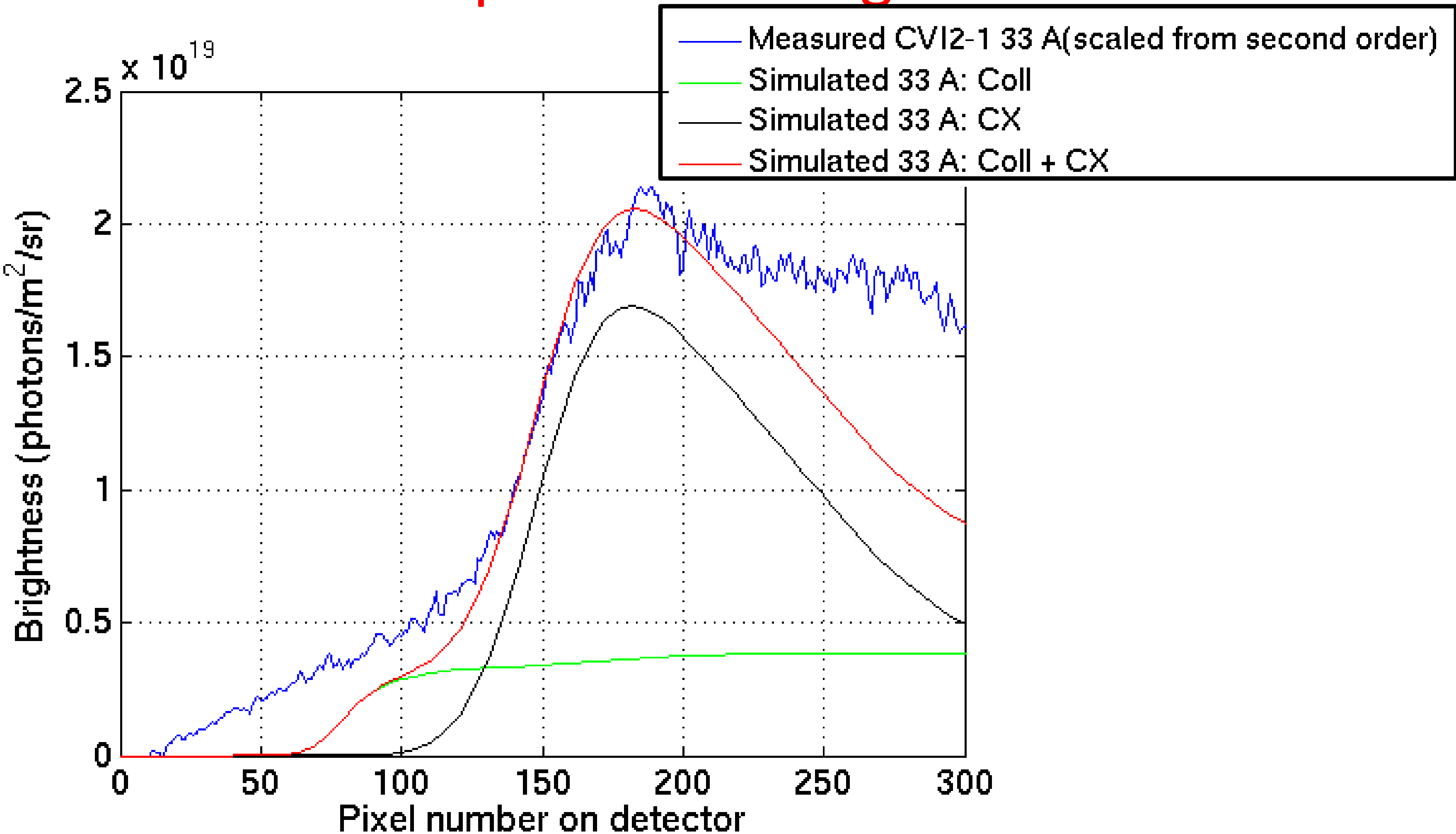

Brightness profile of simulated collisional excitation is expected to fit the experimental data better after including transport in the model

Determination of impurity fractions

Low Z impurity fraction from CX lines

- Closest lines are chosen to mitigate the effect of gain variation of grating and MCP over wavelength
- The brightness of C charge exchange lines obtained from modeling using CHERS data is used as a reference for absolute calibration.
- By the measured brightness of O CX lines (4-3: 293 A and 5-4: 630 A) –

$$\frac{n(O^{8+})}{n(C^{6+})} \sim 12\%$$

- N is observed sometimes in NSTX. However, the CX line of 4-3 transition at 382 A, is blended with Cl line. Thus an upper limit from recent NSTX runs is $n(N^{7+})/n(C^{6+}) < 20\%$.

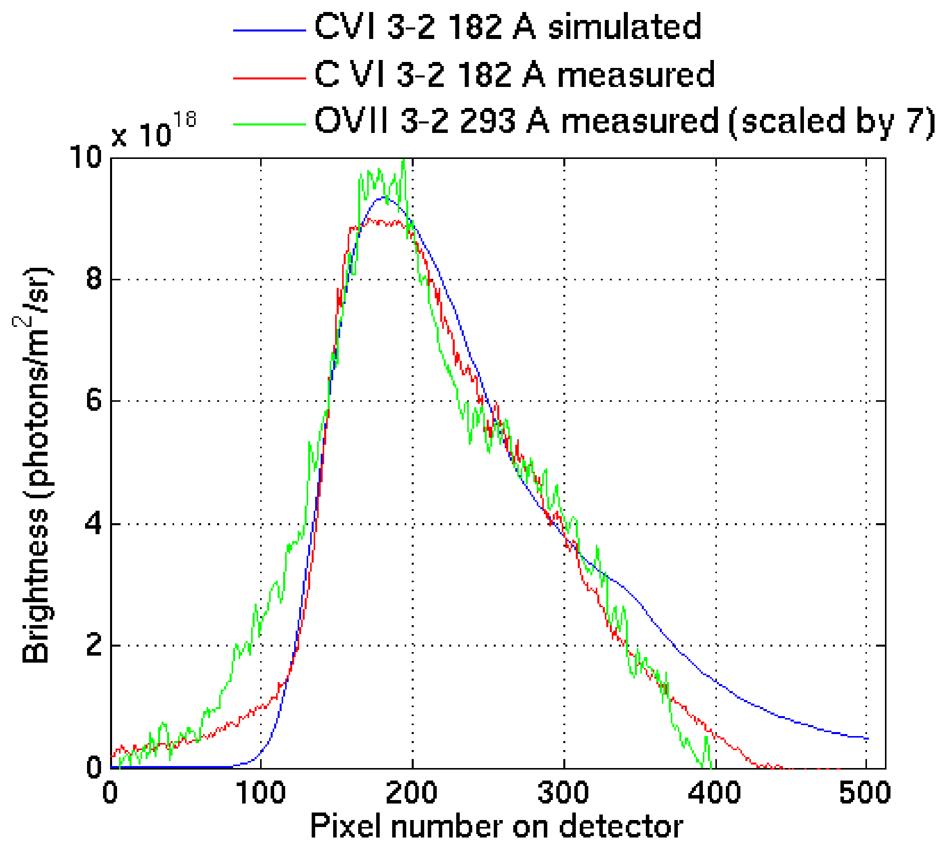

Spectral signature of Li

- Li III (2-1) transition at 135 A is blended with CX lines from C VI (4-2) and N VII(3-2).
- An estimate of the CVI (4-2) brightness compared to the measured brightness is shown →
- The blend makes it extremely difficult to quantify the amount of Li in the plasma
- **SOLUTION:** Extending the spectral range of TGIS to include LI III (3-2) transition at 728 Å. (Planned for 2011).

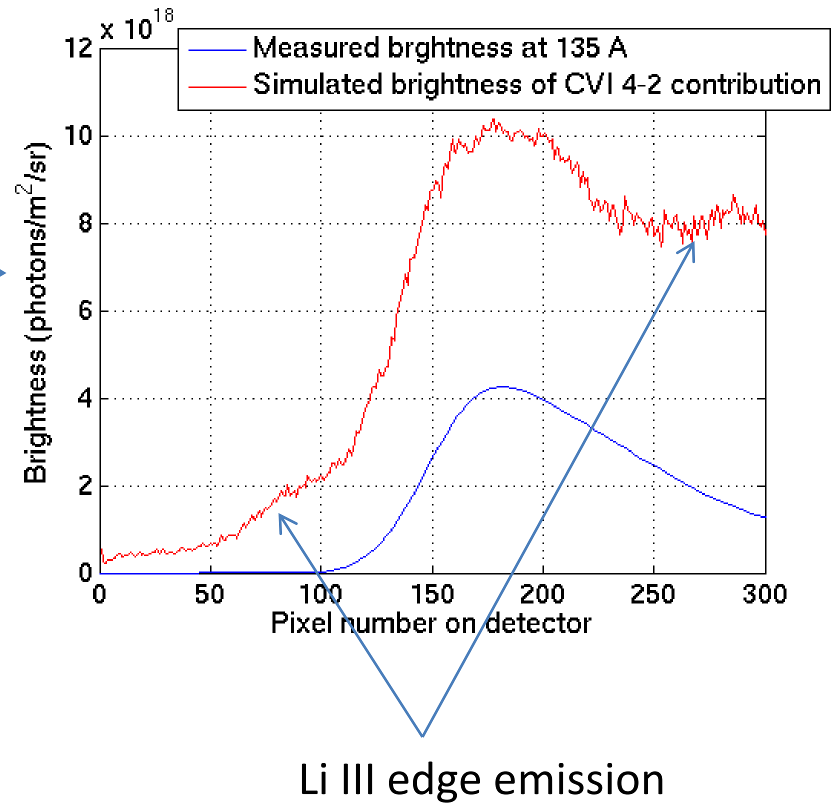

Li Lyman alpha is the most dominant line in loweus spectrometer

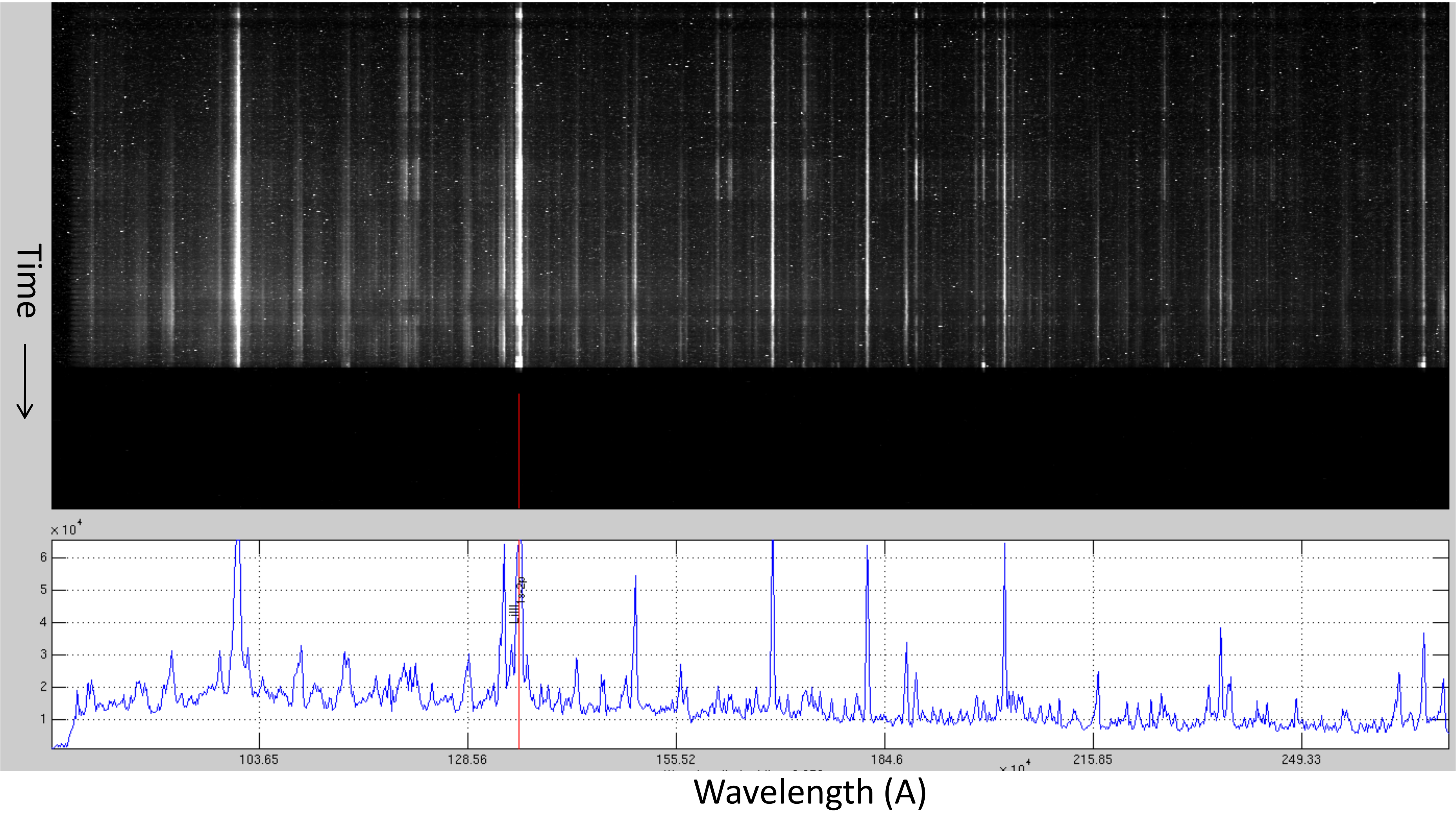

Amount of Cl in the plasma

- The collisional modeling of TGIS suggests n(Cl) ~ 10^{-4} n_e. Change in MCP and grating efficiency over the wide spectral range can account for the presence of higher concentrations of Cl ~ 1 x 10^{-3} n_e , as predicted by ME-SXR.

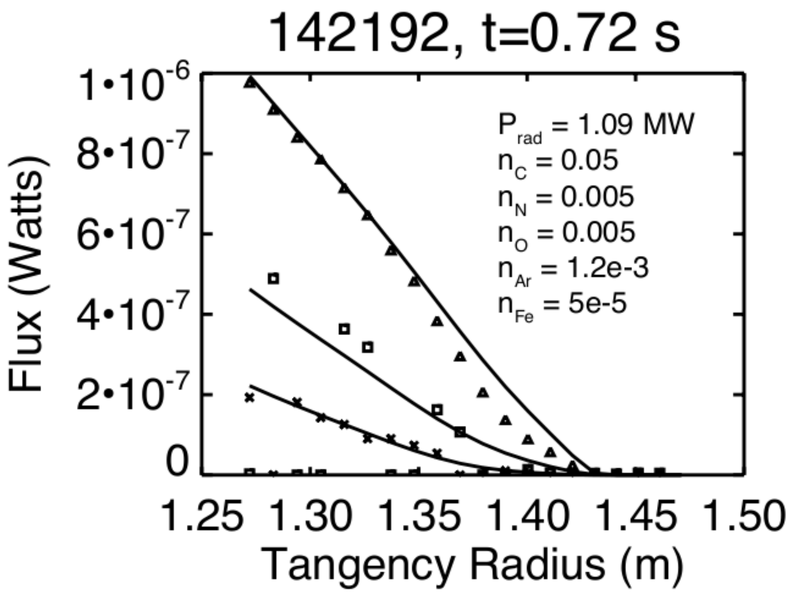

Impurity ratios needed to fit ME-SXR data

TGIS complements high resolution spectrometer

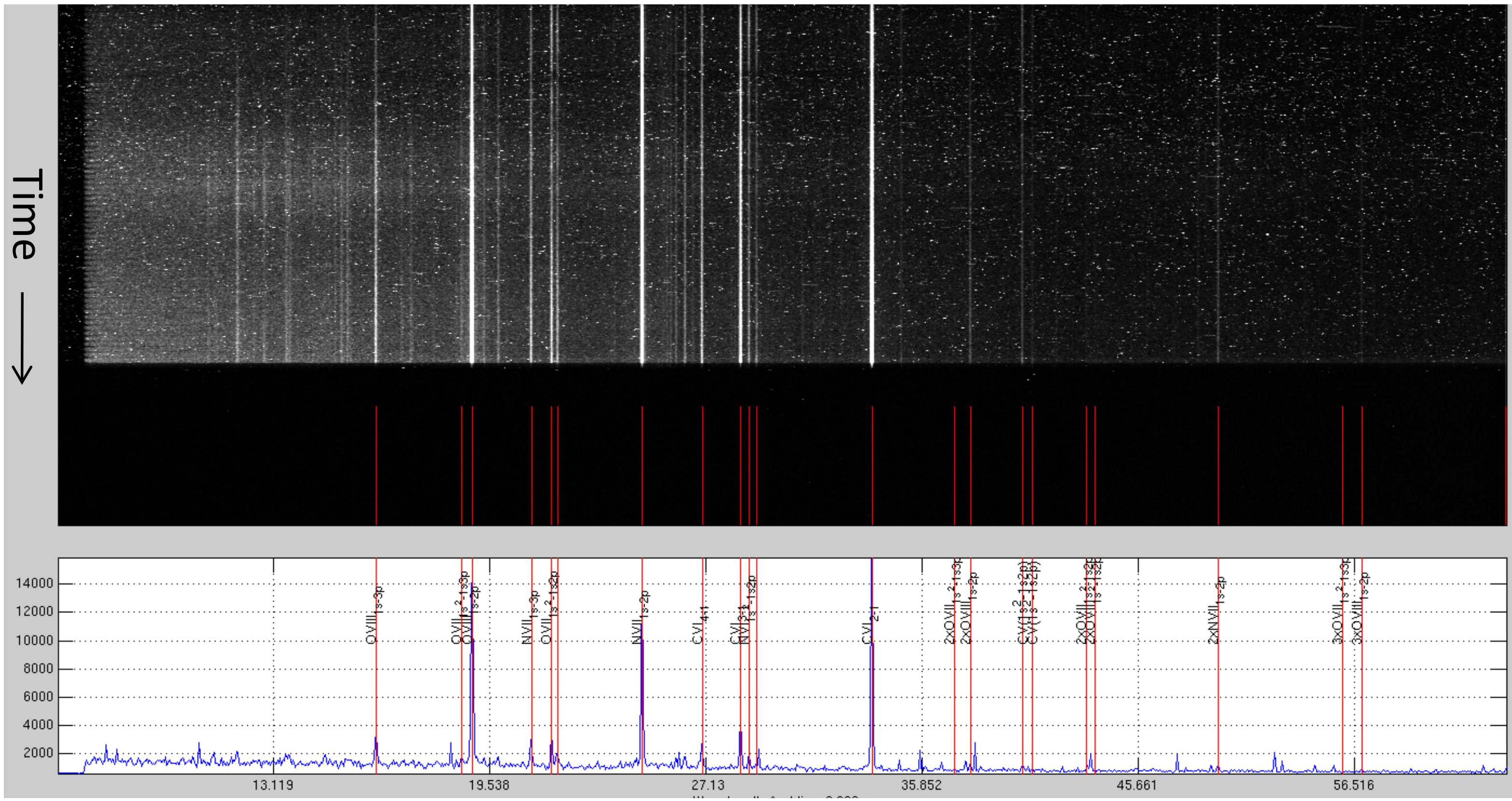

Wavelength (A)

- Data from XEUS is dominated by low Z charge exchange spectra
- Trace Cl does not appear in short wavelengths (explained in the following slides)

SPRED sees strong Cl lines

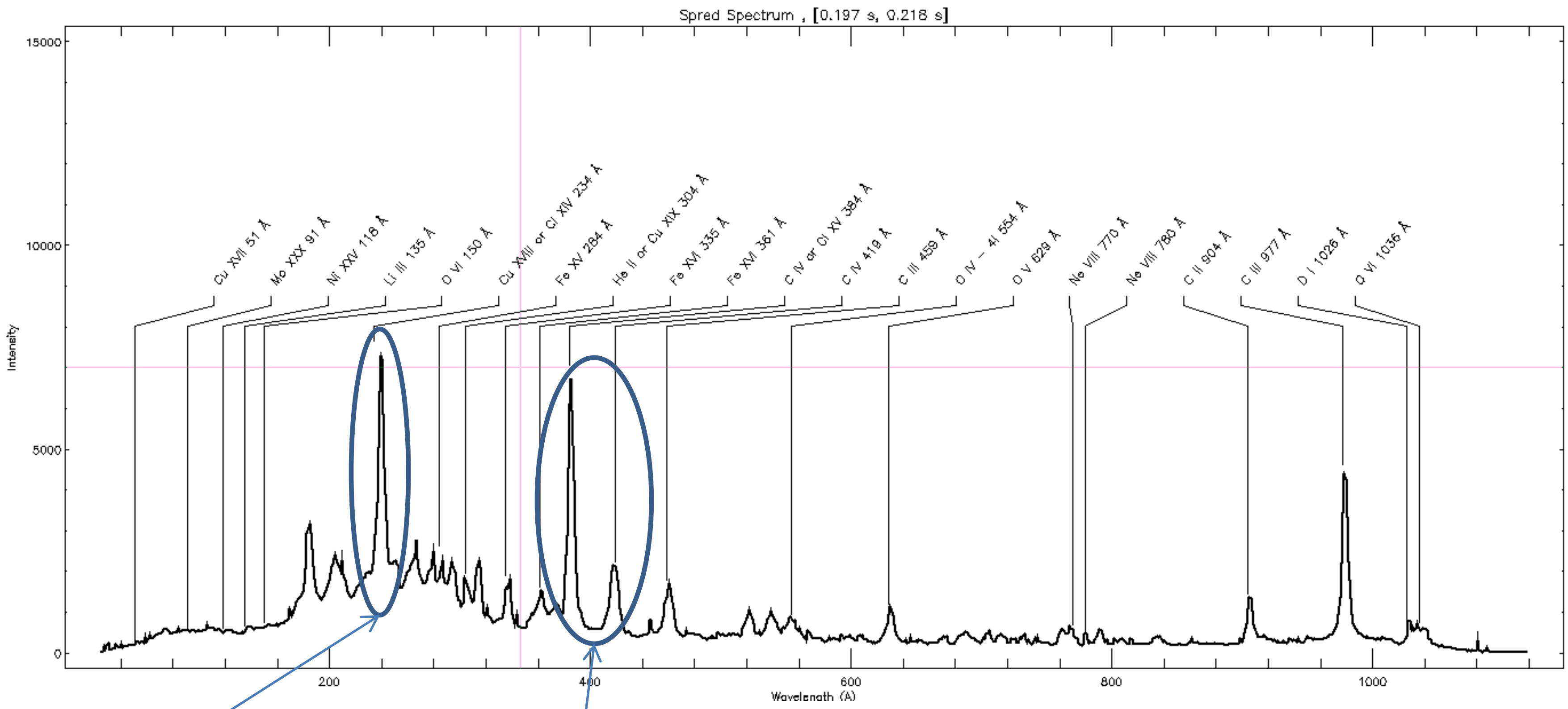

Cl XIV 237 A

Cl XV doublet
384 and 415 A

Synthetic spectra helps explain the absence of Cl lines in shorter wavelengths

- The synthetic spectra of Ar and Fe below illustrates the fact that the brightness of medium Z impurities is highest in the wavelength range (100-500 Å). Thus this wavelength region is better suited to detect medium Z impurities.

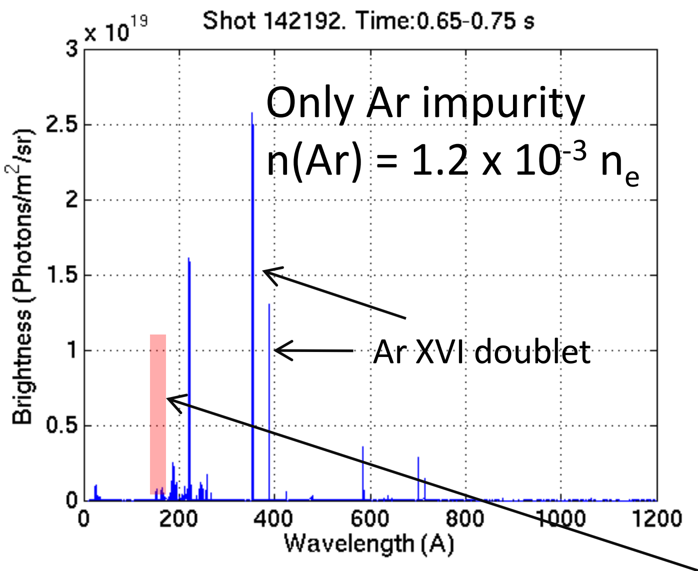

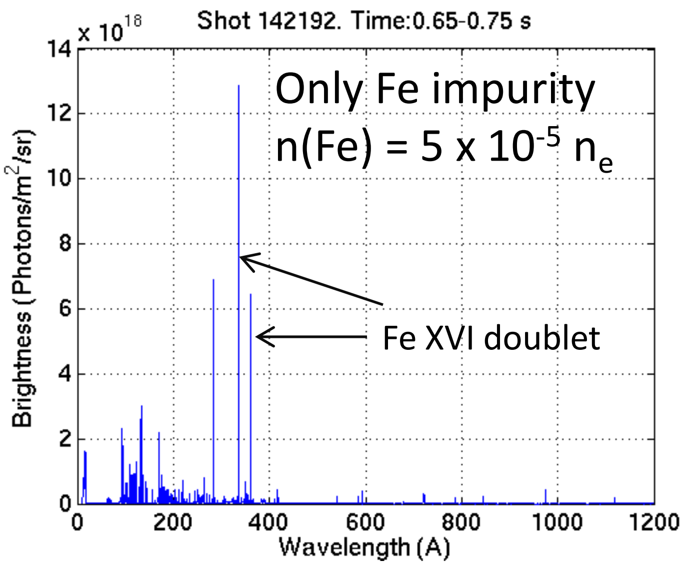

Brightness of CVI (3-2) line
(shown for comparison)

Note: Because of the lack of Cl data in Chianti, Ar lines were simulated instead.

Future work

- Modify the model to generate all the beam stopping cross sections, the charge exchange cross sections and the collisional excitation cross sections using ADAS
- Absolute calibration of grating and MCP at higher wavelengths (planned after the run) will be done against a calibrated Xray CCD camera.

Advanced detectors which can provide better efficiency and time resolution

- Cross delay line anode + MCP

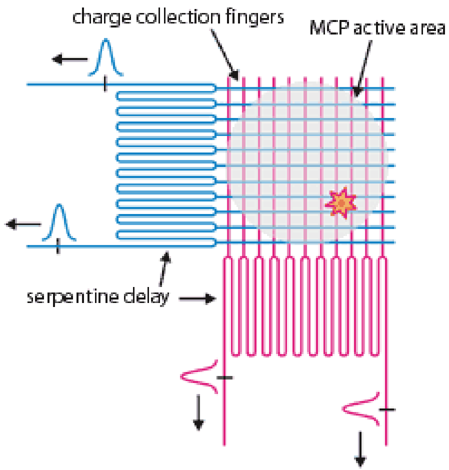

- Direct photon detection

Princeton Instruments, PIXIS-XO: 400B

Summary

- TGIS provides strong constraints on impurity densities needed for ME-SXR modeling.
- Further calibrations will improve the accuracy of the impurity densities.
- Results from the 2010 run indicate that the optimal spectral range for the TGIS on an ST device like NSTX should be 100-800 Å.
- TGIS + ME-SXR make a novel diagnostic suite to provide (n_e ,n_z,T_e) for fusion plasma experiments.
- Direct detection of photons by an X-ray CMOS camera can improve the time and spectral response of TGIS.

Acknowledgements

- Ron Bell
- Jaan Lepson

References

- http://www.chem.queensu.ca/people/faculty/Stolow/Research/Facilities.html
- http://www.sensorsciences.com/

Chlorine (accumulation)

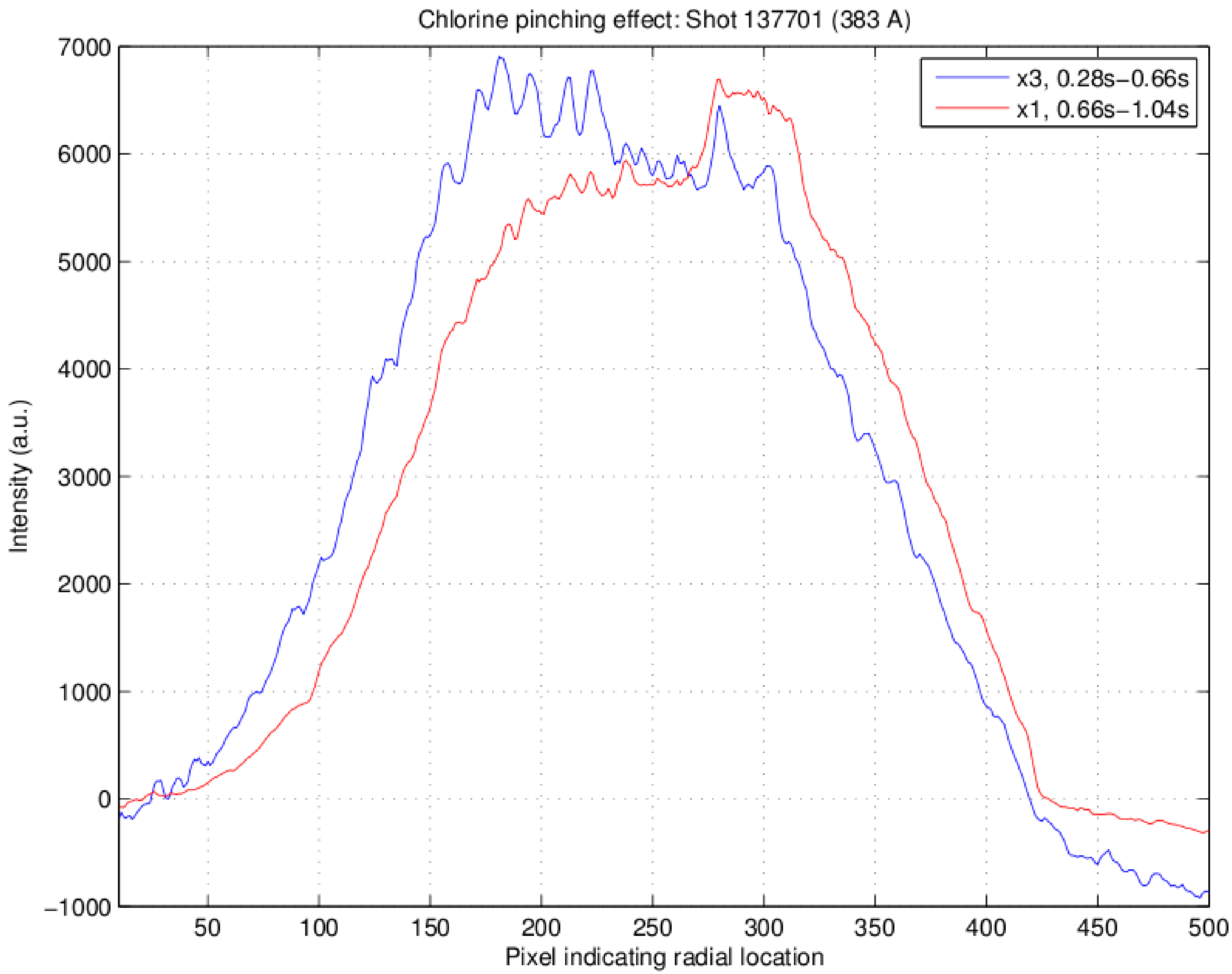

Ohmic shot – spatial profile (edge)

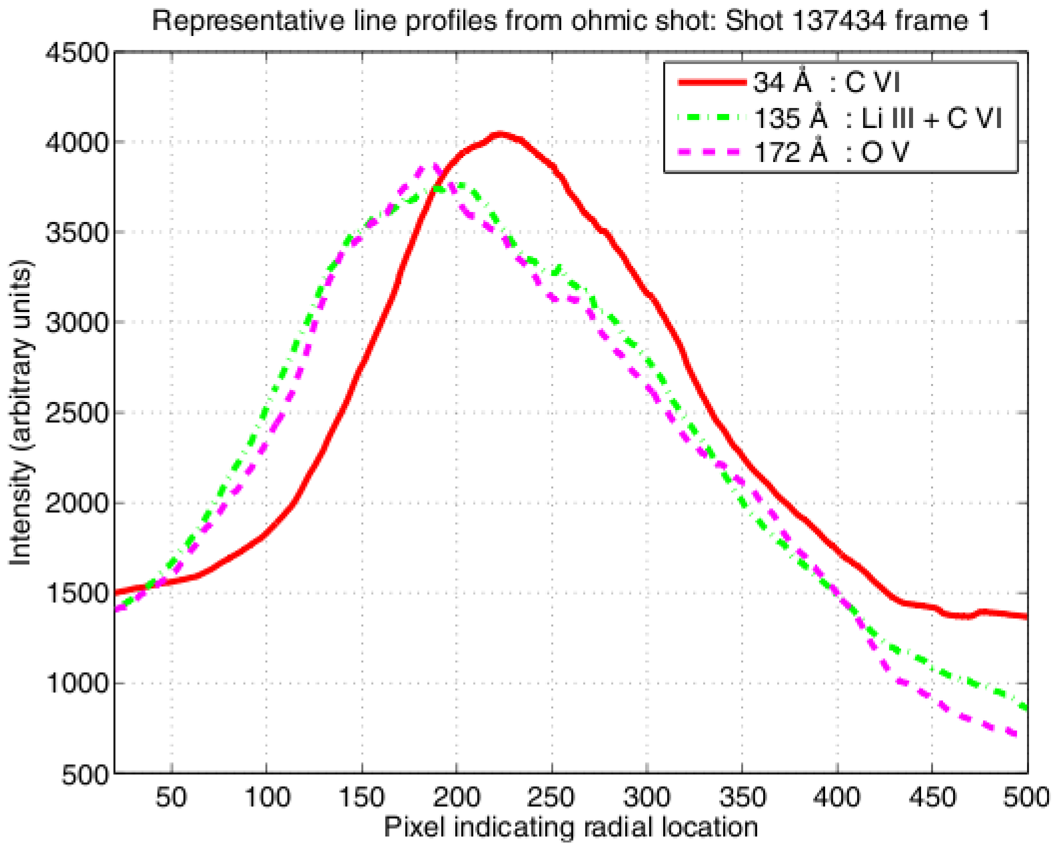

Typical shot – spatial profile (Edge + CX + core)